

EGO TO WORLD: COLLABORATIVE SPATIAL REASONING IN EMBODIED SYSTEMS VIA REINFORCEMENT LEARNING

Heng Zhou^{1,2,*} **Li Kang**^{2,3,*} **Yiran Qin**^{2,‡} **Xiufeng Song**^{2,3} **Ao Yu**¹
Zilu Zhang⁴ **Haoming Song**^{2,3} **Kaixin Xu**^{2,5} **Yuchen Fan**^{2,3}
Dongzhan Zhou² **Xiaohong Liu**³ **Ruimao Zhang**⁶ **Philip Torr**⁷
Lei Bai^{2,†} **Zhenfei Yin**^{7,†}

¹ University of Science and Technology of China ² Shanghai AI Laboratory

³ Shanghai Jiao Tong University ⁴ Beijing University of Posts and Telecommunications

⁵ Fudan University ⁶ Sun Yat-sen University ⁷ University of Oxford

*Equal contributions ‡Project leader †Corresponding author

✉ hengzzzhou@gmail.com 📄 Code 🗄️ HuggingFace 🌐 Project Page

ABSTRACT

Understanding the world from distributed, partial viewpoints is a fundamental challenge for embodied multi-agent systems. Each agent perceives the environment through an ego-centric view that is often limited by occlusion and ambiguity. To study this problem, we introduce the Ego-to-World (E2W) benchmark, which evaluates vision–language model’s ability to fuse heterogeneous viewpoints across three tasks: (i) global counting, (ii) relational location reasoning, and (iii) action-oriented grasping that requires predicting view-specific image coordinates. To address this setting, we propose CoRL, a two-stage framework that combines Chain-of-Thought supervised fine-tuning with reinforcement learning using Group-Relative Policy Optimization. Its core component, the Cross-View Spatial Reward (CVSR), provides dense task-aligned feedback by linking reasoning steps to visual evidence, ensuring coherent cross-view entity resolution, and guiding the model toward correct final predictions. Experiments on E2W show that CoRL consistently surpasses strong proprietary and open-source baselines on both reasoning and perception-grounding metrics, while ablations further confirm the necessity of each CVSR component. Beyond that, CoRL generalizes to external spatial reasoning benchmarks and enables effective real-world multi-robot manipulation with calibrated multi-camera rigs, demonstrating cross-view localization and successful grasp-and-place execution. Together, E2W and CoRL provide a principled foundation for learning world-centric scene understanding from distributed, ego-centric observations, advancing collaborative embodied AI.

1 INTRODUCTION

Recent advances in Vision–Language Models (VLMs) have catalyzed significant progress in embodied intelligence. By grounding natural language within visual perception, VLMs have enabled a diverse range of embodied tasks, from instruction following to interactive manipulation. This progress has spurred extensive research into VLM applications across domains such as robotics (Kang et al., 2025), navigation (Wang et al., 2025b), and spatial reasoning (Zhou et al., 2025; Yin et al., 2025). Nevertheless, the majority of existing methodologies are confined to single-view scenarios, where perception is limited to an ego-centric or a fixed global viewpoint. Such a constraint inherently leads to incomplete scene understanding and restricted reasoning capabilities.

In many real-world applications, multiple heterogeneous agents, such as cooperative service robots in domestic environments (Forlizzi & DiSalvo, 2006) or Vehicle-to-Everything (V2X) systems in autonomous driving, operate concurrently (Liu et al., 2023). Throughout this work, “multi-agent” refers to physically separate robots, each equipped with its own ego-centric sensor and limited

field of view, rather than to multi-agent planning or decision-making. In these settings, multi-agent coordination is not merely beneficial but essential. A solitary viewpoint is fundamentally susceptible to occlusions and partial observations, whereas integrating complementary perspectives from multiple agents can provide richer contextual understanding. As illustrated in Figure 1, cross-view compositional reasoning empowers agents to surmount these limitations and execute spatially grounded actions with high fidelity.

From a practical standpoint, relying on a single global camera is often infeasible: global cameras require careful placement, suffer from occlusions, and cannot flexibly cover diverse interaction zones. In contrast, ego-centric sensors naturally accompany each agent, providing *dynamic*, *task-relevant*, and *complementary* observations that yield richer spatial coverage. From a reasoning perspective, multi-view information is more expressive than any single global shot: while a global viewpoint may miss critical details due to perspective distortion or object self-occlusion, aggregating multiple close-range ego-centric views reduces ambiguity and significantly improves spatial grounding.

However, achieving such reasoning capabilities is profoundly challenging, as it necessitates the integration of heterogeneous viewpoints, the resolution of cross-view ambiguities, and the alignment of overlapping observations to construct a coherent scene representation.

To bridge this critical gap, we investigate the problem of collaborative spatial reasoning in multi-agent embodied systems. We formalize a novel setting wherein each agent contributes its partial, ego-centric observations, and the VLM must integrate these disparate inputs to perform complex spatial reasoning and perception tasks. To this end, we introduce the **Collaborative Spatial Reasoning Reinforcement Learning (CoRL)** framework, which is augmented by a novel **Cross-View Spatial Reward (CVSR)**. The CVSR is designed to explicitly incentivize policies that: (i) consistently localize objects across different viewpoints, (ii) effectively fuse complementary ego-centric information, and (iii) maximize collective scene coverage. By shaping the learning signal around these core principles of spatial grounding, CVSR compels the VLM to transcend single-view perception and develop robust collaborative spatial reasoning abilities. Through systematic comparisons of alternative training paradigms, we demonstrate that our proposed Supervised Fine-Tuning (SFT) followed by Reinforcement Learning (RL) pipeline, empowered by CVSR, consistently achieves state-of-the-art performance on collaborative perception tasks.

In summary, our contributions are threefold:

- ◊ We pioneer the formalization of collaborative perception and reasoning with VLMs in multi-agent embodied systems, and introduce the E2W benchmark specifically tailored for this setting.
- ◊ We propose the CoRL framework, featuring the novel Cross-View Spatial Reward (CVSR), which explicitly incentivizes the fusion of ego-centric views and enhances spatial grounding.
- ◊ We empirically validate the effectiveness and generalizability of our approach, consistently showing substantial improvements over strong baselines.

2 RELATED WORK

Embodied Multi-Agent Cooperation. Coordination among multiple agents is a fundamental challenge in embodied AI. Research in this domain has historically focused on high-level task allocation Obata et al. (2024); Wang et al. (2024); Liu et al. (2025a) and joint decision-making Zhang et al. (2023a); Wang et al. (2025a). More recently, the advent of Large Language Models (LLMs) has catalyzed progress in multi-agent collaboration, enabling sophisticated distributed planning and communication strategies Bo et al. (2024); Guo et al. (2024); Nasiriany et al. (2024); Zhou et al. (2023). However, a primary limitation of these LLM-based approaches is their reliance on symbolic or textual representations, which are detached from the visual world. This detachment restricts their capacity to handle perceptual ambiguities and perform fine-grained spatial reasoning. While a few pioneering studies have started to integrate Vision-Language Models (VLMs) into multi-agent systems Wang et al. (2025b); Zhang et al. (2024a); Kang et al. (2025; 2026); Qin et al. (2025c), they typically treat each agent’s viewpoint in isolation or default to single-view reasoning. For instance, COMBO Zhang et al. (2024a) assumes a shared global state rather than distributed ego-centric fusion, sidestepping the need for cross-view entity resolution. In stark contrast, our work directly confronts

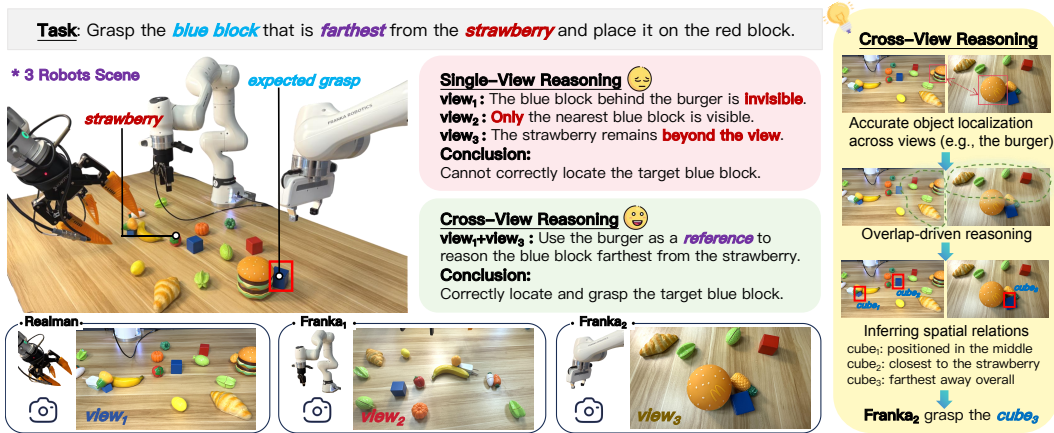


Figure 1: An illustration of collaborative spatial reasoning in embodied systems. Reasoning from a single viewpoint fails due to occlusions or a limited field of view. In contrast, cross-view compositional reasoning integrates multiple perspectives to correctly localize and grasp the target object—the blue block farthest from the strawberry.

this limitation by proposing a framework centered on compositional, cross-view reasoning for deeper and more effective collaboration.

Spatial Understanding. Spatial understanding—the ability to parse intricate geometric configurations, spatial layouts, and object interrelations from diverse visual inputs—is critical for intelligent systems across a wide range of domains, from geometric problem-solving Gao et al. (2023); Shi et al. (2024); Zhang et al. (2024b) to embodied robotics Hu et al. (2023); Ji et al. (2025). To bolster the spatial reasoning capabilities of VLMs, recent works have explored increasingly advanced training methodologies. Techniques such as multi-stage supervision with Chain-of-Thought (CoT) prompting Xu et al. (2024); Wei et al. (2022) and reinforcement learning (RL) with carefully engineered reward mechanisms Guo et al. (2025) have yielded significant gains. Subsequent research has further underscored the importance of highly tailored reward designs for complex visual reasoning tasks Liu et al. (2025b;c); Tan et al. (2025). MindCube Yin et al. (2025) represents a notable step in this direction, showing that VLMs can infer hidden spatial layouts from a few static views. However, their setting fundamentally differs from ours. While it focuses on mental reconstruction of hidden layouts from a few static viewpoints, our work targets cross-view reasoning for embodied manipulation, where multiple distributed robots contribute heterogeneous ego-centric observations over time. We further study this capability across diverse embodied task settings, as detailed in Section 3. Building upon this line of inquiry, our work addresses the distinct and even more complex challenge of *multi-agent* spatial understanding. Here, the central problem is to synthesize a globally coherent and semantically consistent scene representation from fragmented, ego-centric observations. This necessitates not only unifying disparate multi-view visual data but also enforcing strong and robust spatial consistency across multiple, partially overlapping perspectives.

Reinforcement Learning for Visual Reasoning. Reinforcement Learning (RL) has emerged as a powerful and versatile paradigm for training intelligent agents that reason from high-dimensional visual data Zhang et al. (2025). Moving beyond the static nature of supervised pretraining, RL enables models to learn through direct and interactive environmental engagement, optimizing their policies via reward-driven feedback Liu et al. (2025b); Tan et al. (2025); Sarch et al. (2025); Chen et al. (2025). Foundational applications in perception-driven tasks, such as navigation Zhu et al. (2017) and manipulation Zhou et al. (2025); Kang et al. (2025), have demonstrated RL’s strong efficacy in tightly coupling perception and action. More recently, the field has progressed toward structured reward designs for multi-modal reasoning, incorporating mechanisms like CoT guidance Zhang et al. (2024c) and geometric consistency constraints Jiang & Lu (2024) to further enhance embodied decision-making performance. Despite these advances, the predominant focus of RL-based visual reasoning has remained on single-agent, single-image settings, leaving multi-view reasoning largely underexplored. Recent efforts such as VLA-R1 Ye et al. (2025) and VLM-R1 Shen et al. (2025)

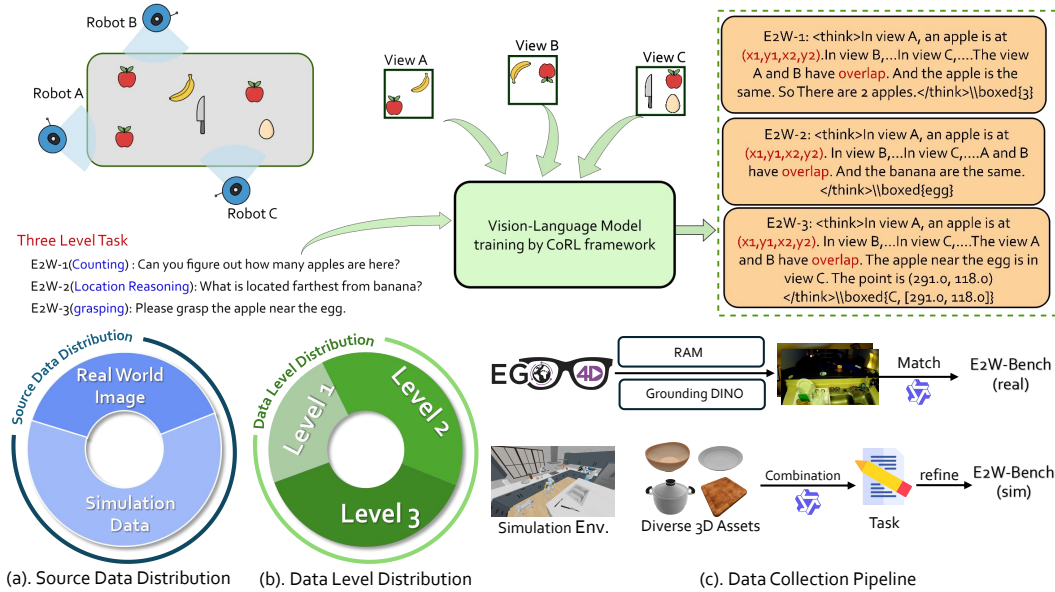


Figure 2: **Overview of the Ego-to-World (E2W) Benchmark.** **Top:** Multiple agents (Robot A, B, C) each provide partial ego-centric views of a shared scene. The vision language model trained with our CoRL framework integrate these complementary perspectives to solve three tasks: Counting (E2W-1), Location Reasoning (E2W-2), and Grasping (E2W-3). **Bottom:** The benchmark combines diverse real and simulated data and organizes them into varying complexity levels.

apply RL to vision-language models, yet they operate exclusively on single-agent policies without cross-view reasoning or distributed observation fusion. Moreover, existing RL formulations rarely address how visual evidence from multiple ego-centric viewpoints should be aligned, fused, and jointly grounded. Our framework extends this paradigm to the multi-agent, multi-view context, introducing a novel and unified reward structure designed explicitly to foster collaborative spatial reasoning.

3 EGO-TO-WORLD TASK

To systematically evaluate collaborative spatial reasoning, we introduce the *Ego-to-World Benchmark (E2W-Bench)*, which operationalizes a multi-agent, multi-view paradigm. As shown in Figure 2, multiple robotic agents capture partial ego-centric observations of a shared 3D environment. The central challenge for a Vision-Language Model is to integrate these fragmented perspectives into a coherent global scene representation and to answer natural-language queries or perform action-oriented predictions. E2W-Bench consists of two categories of tasks: spatial reasoning QA (E2W-1, E2W-2) and perception for grasping (E2W-3). Further dataset details are provided in Appendix D.

E2W-1 (Counting). This task evaluates the ability to aggregate object instances across overlapping views and output an accurate global count.

E2W-2 (Location Reasoning). Here the model must infer spatial relations among objects that never co-occur in a single view, requiring cross-view reasoning to answer correctly in natural language.

E2W-3 (Grasping). Unlike the QA tasks, E2W-3 requires action-oriented predictions. The model must translate a language command involving spatial relations into precise 2D coordinates within specific agent’s viewpoint, thereby linking compositional reasoning to downstream robotic manipulation.

Together, these tasks provide a comprehensive benchmark that jointly evaluates high-level symbolic reasoning, fine-grained visual grounding, and embodied spatial referring across diverse scenarios. E2W-Bench comprises over 100k simulated and 60k real-world samples spanning more than 15k scenes and 50+ object categories. Train and test sets are scene-disjoint, ensuring that no scene

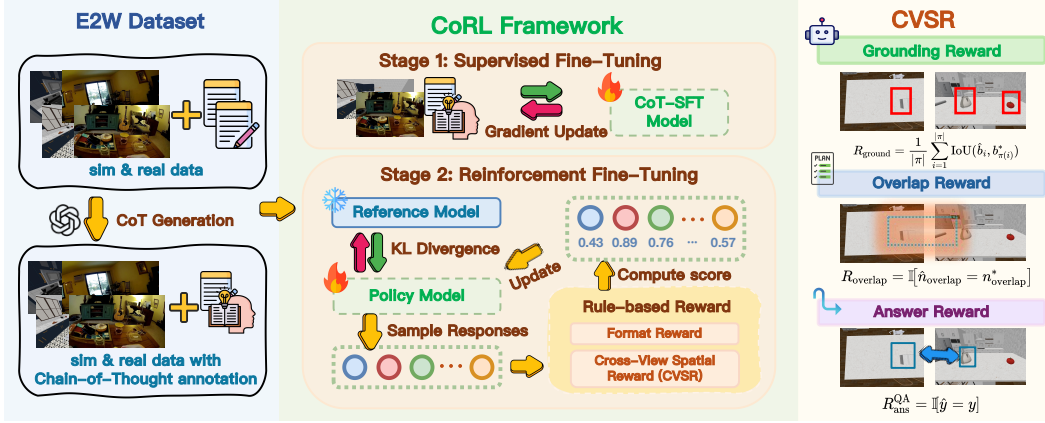


Figure 3: **CoRL framework.** The model is first initialized via supervised fine-tuning (SFT) on Chain-of-Thought annotations, then refined with reinforcement learning (RL). During RL, the policy is optimized with an format reward and the Cross-View Spatial Reward (CVSR), which supplies dense feedback on cross-view fusion and spatial consistency, guiding robust collaborative reasoning.

configuration appears in both splits. By explicitly linking abstract reasoning to actionable predictions, E2W-Bench offers a rigorous testbed for multi-view understanding.

4 METHODS

4.1 OVERVIEW

We present *CoRL* (Collaborative Spatial Reasoning Reinforcement Learning), a framework that equips Vision–Language Models (VLMs) with collaborative perception and reasoning capabilities in multi-agent embodied settings. A central VLM aggregates and reasons over partial, ego-centric observations streamed by multiple agents, producing task-specific outputs under a unified interface. The overall architecture is shown in Figure 3.

4.2 PROBLEM FORMULATION

Consider a shared environment \mathcal{E} populated by N embodied agents $\mathcal{A} = \{a_1, \dots, a_N\}$. At a given time, each agent a_i observes an ego-centric RGB image $I_i \in \mathbb{R}^{H \times W \times 3}$. All agents receive a common natural-language query Q . A central VLM implements a policy π_θ parameterized by θ that consumes the multi-view input and the query to produce a prediction

$$\hat{y} = \pi_\theta(\{I_i\}_{i=1}^N, Q), \quad (1)$$

where \hat{y} is either a textual response (for counting and relational reasoning) or a pair of image-plane coordinates (for grasping).

Training is cast as maximizing the expected task reward over a dataset \mathcal{D} of instances $(\{I_i\}, Q, y)$ with ground-truth label y :

$$\max_{\theta} \mathbb{E}_{(\{I_i\}, Q, y) \sim \mathcal{D}} [R(\hat{y}, y)]. \quad (2)$$

The reward function R evaluates the quality of \hat{y} against y and is central to our method; its design is detailed in Section 4.4.

4.3 CORL TRAINING PIPELINE

CoRL is trained in two stages: supervised fine-tuning for cold start, followed by reinforcement learning.

Supervised Fine-Tuning. We initialize π_θ with SFT on CoT-augmented data. Each training tuple is (x, q, r, a) , where x denotes the multi-view inputs, q is the query, r is the intermediate reasoning trace, and a is the final answer. Let $y = [r, a]$ be the concatenated target sequence. The SFT objective is the usual next-token log-likelihood:

$$\mathcal{L}_{\text{SFT}} = -\mathbb{E}_{(x,q,r,a) \sim \mathcal{D}} \sum_{t=1}^{|y|} \log \pi_\theta(y_t \mid x, q, y_{<t}). \quad (3)$$

This yields an initial policy π_{SFT} (denoted π_0) that provides a strong starting point for RL.

Reinforcement Learning Fine-Tuning. After SFT initialization, we further optimize the policy with *Group Relative Policy Optimization* (GRPO). GRPO improves stability and sample efficiency by normalizing rewards within each sampled group of candidate responses, thereby computing *group-relative advantages* that reduce variance and sharpen credit assignment.

Concretely, for an input $u = (x, q)$, we draw G candidate responses $\{y_j\}_{j=1}^G$ from the current policy π_θ and score each with a reward R_j (Section 4.4). GRPO computes the empirical mean \bar{R} and standard deviation σ_R of the rewards and defines a standardized advantage for each candidate:

$$\mathcal{A}_j = \frac{R_j - \bar{R}}{\sigma_R}. \quad (4)$$

This group-relative normalization emphasizes responses that outperform their peers, rather than absolute reward magnitude, and thus stabilizes training.

To update the policy, we first define the probability ratio between the current policy π_θ and the reference policy π_0 from SFT:

$$r_j(\theta) = \frac{\pi_\theta(y_j \mid u)}{\pi_0(y_j \mid u)}. \quad (5)$$

The core of the GRPO objective is a clipped surrogate function, which constrains the policy update step size. This objective is defined as:

$$\mathcal{L}^{\text{CLIP}}(\theta) = \mathbb{E}_u \left[\sum_{j=1}^G \min \left(r_j(\theta) \mathcal{A}_j, \text{clip}(r_j(\theta), 1 - \epsilon, 1 + \epsilon) \mathcal{A}_j \right) \right], \quad (6)$$

where ϵ is a hyperparameter that defines the clipping range.

The final policy parameters are updated by maximizing the full GRPO objective, which incorporates a KL divergence penalty to further regulate the policy update:

$$\mathcal{J}(\theta) = \mathcal{L}^{\text{CLIP}}(\theta) - \beta \text{D}_{\text{KL}}(\pi_\theta(\cdot \mid u) \parallel \pi_0(\cdot \mid u)), \quad (7)$$

where π_0 is the SFT-initialized reference policy and $\beta > 0$ regulates the trust region enforced by the KL regularizer. This formulation allows CoRL to directly optimize spatial reasoning rewards while preserving stability and sample efficiency, fully leveraging the group-relative advantage mechanism within a robust PPO-style optimization framework.

4.4 CROSS-VIEW SPATIAL REWARD (CVSR) DESIGN

The total reward combines an output-format component with a cross-view spatial component:

$$R = \lambda_1 R_{\text{format}} + \lambda_2 R_{\text{CVSR}}, \quad \lambda_1, \lambda_2 > 0. \quad (8)$$

Output-Format Reward R_{format} . To ensure interpretability and reliable parsing, the model receives a binary reward for structural correctness. Specifically, the intermediate reasoning must be enclosed in `<think>...</think>` tags and the final answer must appear in a designated box; success yields $R_{\text{format}} = 1$, otherwise 0. This encourages the model to articulate a reasoning trace prior to committing to an answer.

Cross-View Spatial Reward R_{CVSR} . CVSR delivers dense feedback targeted at collaborative spatial reasoning. It aggregates three components:

$$R_{\text{CVSR}} = w_{\text{ground}} R_{\text{ground}} + w_{\text{overlap}} R_{\text{overlap}} + w_{\text{ans}} R_{\text{ans}}, \tag{9}$$

with nonnegative weights $w_{\text{ground}}, w_{\text{overlap}}, w_{\text{ans}}$.

(i) *Grounding reward R_{ground} .* To align reasoning with visual evidence, the model is prompted to emit bounding boxes for key objects referenced in its chain of thought. Let $\hat{B} = \{\hat{b}_i\}_{i=1}^m$ be predicted boxes and $B^* = \{b_j^*\}_{j=1}^n$ ground-truth boxes. We compute an optimal bipartite matching σ via the Hungarian algorithm that maximizes total IoU, and define

$$R_{\text{ground}} = \frac{1}{|\sigma|} \sum_{i=1}^{|\sigma|} \text{IoU}(\hat{b}_i, b_{\sigma(i)}^*), \tag{10}$$

which provides a dense localization signal.

(ii) *Overlap accuracy R_{overlap} .* To incentivize cross-view entity resolution, the model must report the number of unique object instances that appear in more than one view, denoted \hat{n}_{overlap} . Comparing to the ground truth n_{overlap}^* yields

$$R_{\text{overlap}} = \mathbb{I}[\hat{n}_{\text{overlap}} = n_{\text{overlap}}^*], \tag{11}$$

encouraging the model to distinguish redundant from complementary observations before global aggregation.

(iii) *Answer correctness R_{ans} .* This term evaluates task completion and is defined per task type. For counting and location reasoning (textual outputs),

$$R_{\text{ans}}^{\text{QA}} = \mathbb{I}[\hat{y} = y]. \tag{12}$$

For grasping (coordinate output $\hat{y} = (\hat{u}, \hat{v})$ with ground truth $y = (u, v)$), we use a distance-shaped reward

$$R_{\text{ans}}^{\text{grasp}} = \max\left(0, 1 - \frac{\|\hat{y} - y\|_2}{d_{\text{max}}}\right), \tag{13}$$

where d_{max} is a normalization radius. While R_{ground} and R_{overlap} shape intermediate spatial reasoning, R_{ans} enforces correctness of the final output.

5 EXPERIMENTS

5.1 EXPERIMENTAL SETUP

Simulation Environment and Data Generation. The simulated portion of E2W-Bench is constructed using RoboFactory Qin et al. (2025a), a framework for embodied multi-agent manipulation built on ManiSkill3 Tao et al. (2024). Chain-of-Thought (CoT) annotations for supervised fine-tuning are generated through a three-step pipeline: ground-truth bounding boxes are first extracted from simulator metadata, spatial relations are then computed programmatically, and finally reasoning traces are assembled from structured templates. This ensures high-quality, consistent annotations without relying on manual labeling.

Baselines and Protocol. We compare **CoRL** with (i) proprietary VLMs: GPT-5 OpenAI (2025), Gemini-2.5-Pro Comanici et al. (2025), and Doubao-Seed-1.6 Seed (2025); (ii) open-source VLMs: GLM-4.5V Team et al. (2025), Qwen2.5-VL-32B Bai et al. (2025), LLaMA-3.2-11b-vision-instruct Dubey et al. (2024), SpaceQwen3B Yang et al. (2025); and (iii) fine-tuned variants on Qwen2.5-VL-Instruct Bai et al. (2025) backbones (3B/7B): +SFT, +RL-ZERO (RL from scratch). All baseline models are evaluated with zero-shot inference under identical prompts and input aggregation protocol, ensuring a fair comparison. Complete training details and prompt templates are provided in the Appendix.

Table 1: **Performance on E2W-Bench.** Tasks are grouped into Reasoning (accuracy, %) and Perception (score, %). (S) = simulation, (R) = real-world. **Best** in bold, second best underlined.

Model	Reasoning (Acc)				Perception (Score)		
	E2W-1	E2W-2(S)	E2W-2(R)	Avg.	E2W-3(S)	E2W-3(R)	Avg.
<i>Closed Source Models</i>							
GPT-5	42.5	48.5	72.5	54.50	50.43	12.02	31.23
Doubao-Seed-1.6	35.0	40.0	46.0	40.33	16.60	5.26	10.93
Gemini-2.5-Pro	32.5	42.5	50.0	41.67	35.98	10.15	23.07
<i>Open Source Models</i>							
GLM-4.5v	34.5	29.0	56.0	39.83	2.78	0.84	1.81
SpaceQwen-3B	21.5	6.0	60.0	29.17	16.15	5.07	10.61
LLaMA-3.2-11b	16.5	12.5	17.5	15.50	7.78	3.38	5.58
Qwen2.5VL-32B	21.5	28.0	37.0	28.83	31.25	9.16	20.21
<i>Qwen2.5VL-3B</i>							
Zero-shot	22.0	15.5	58.0	31.83	24.08	7.48	15.78
+SFT	47.0	63.0	84.0	64.67	93.00	<u>42.06</u>	67.53
+RL-ZERO	23.0	39.5	83.5	48.67	50.63	8.02	29.33
+CoRL (Ours)	<u>59.0</u>	75.5	<u>86.0</u>	<u>73.50</u>	96.30	41.82	<u>69.06</u>
<i>Qwen2.5VL-7B</i>							
Zero-shot	17.0	17.0	64.5	32.83	28.83	5.78	17.31
+SFT	44.5	<u>88.0</u>	84.5	72.33	90.99	40.76	65.88
+RL-ZERO	16.0	56.0	82.5	51.50	92.60	11.65	52.13
+CoRL (Ours)	61.0	97.0	90.0	82.67	<u>95.69</u>	44.32	70.01

Implementation Details. All models are built on the Qwen2.5-VL-Instruct backbone. During the SFT stage, we train for 3 epochs with a cosine-decay learning rate schedule (peak 2×10^{-5}) and a per-device batch size of 4, accumulating gradients over 4 steps. For RL fine-tuning with GRPO, we sample $G = 8$ candidate responses per input, set the clipping range $\epsilon = 0.2$, the KL coefficient $\beta = 0.04$, and the reward weights $\lambda_1 = 0.1$, $\lambda_2 = 1.0$. The normalization radius d_{\max} for the grasping reward is set to 100 pixels. RL training runs for 200 steps with a learning rate of 1×10^{-6} . All experiments are conducted on $8 \times$ NVIDIA H200.

Evaluation Benchmarks and Metrics. We conduct our primary evaluation on the proposed **E2W-Bench**, which comprises the Counting, Location Reasoning, and Grasping tasks detailed in Section 3. For the QA-based tasks (Counting and Location Reasoning), we report exact match accuracy. For Grasping, we report a normalized score from 0 to 100, calculated based on the Euclidean distance between the predicted and ground-truth coordinates, consistent with the task’s reward function defined in our methodology. To further assess the generalization capabilities of our approach, we also report performance on the external Where2Place dataset, a standard testbed for spatial reasoning. A detailed description of dataset statistics, implementation specifics, and evaluation protocols is provided in the Appendix D.

5.2 MAIN RESULTS ON E2W-BENCH

Our main findings on the E2W-Bench are summarized in Table 1. The results show a clear performance hierarchy across the different model categories. In a zero-shot setting, proprietary models like GPT-5 establish the strongest baseline, significantly outperforming open-source VLMs, which generally struggle with the benchmark’s complex multi-view demands. The model fine-tuned on E2W-Bench training set, demonstrate the efficacy of our proposed training pipeline. The SFT-only

Table 2: **Ablation of CVSR Components.** Results of CoRL-7B on E2W-Bench.

Setting	E2W-1	E2W-2(S)	E2W-3(S)
CoRL (CVSR)	61.0	97.0	95.69
<i>Ablation</i>			
w/o R_{ans}	10.5	15.5	40.32
w/o R_{ground}	50.5	90.5	74.32
w/o R_{overlap}	56.5	90.0	84.31
w/o R_{format}	58.5	93.0	89.31

Table 3: **Single-view vs. Multi-view.** Performance on E2W-Bench.

Setting	E2W-1	E2W-2(S)
<i>7B Backbone</i>		
Single-view	34.0	54.0
Multi-view	61.0	97.0
<i>3B Backbone</i>		
Single-view	36.5	51.5
Multi-view	59.0	75.5

models establish a very strong performance level, while the full CoRL (SFT+RL) framework consistently achieves the highest scores across both 3B and 7B model scales. Notably, the RL-ZERO model performs poorly, underscoring the necessity of a supervised warm-up phase to stabilize optimization and provide a reliable initialization. This observation further highlights the complementary nature of SFT and RL, where supervised fine-tuning imparts essential reasoning priors and reinforcement learning subsequently refines them toward task-specific objectives.

A deeper analysis across task categories reveals distinct performance patterns. On the **Reasoning** tasks (E2W-1 and E2W-2), which require aggregating abstract information across views, the largest models show some inherent capability. However, the RL stage of our CoRL framework provides a crucial advantage, refining the model’s ability to resolve cross-view ambiguities and synthesize a coherent global state, as evidenced by the superior scores of CoRL models. The most pronounced gap emerges in the **Perception Grounding** task (E2W-3). Here, nearly all zero-shot models fail to produce reliable coordinates, exposing a weakness in fine-grained spatial grounding. In contrast, our models excel, thanks to explicit supervision in our dataset and, for CoRL, the targeted policy optimization from CVSR’s grounding and consistency rewards, which shape the model toward physically precise and reliable outputs.

We also note an important observation regarding the performance gap between simulated and real-world subsets. Scores on the real-world subset (R) are generally higher than on the simulated subset (S), which may appear counter-intuitive. This is by design: the simulation subset features deliberately challenging configurations including cluttered scenes, severe occlusions, and adversarial spatial layouts, whereas the real-world subset is curated with cleaner visibility. Thus the difficulty gap, rather than domain mismatch, primarily explains the observed score difference.

Beyond task-level accuracy, a critical capability that CoRL acquires is *cross-view entity resolution*, determining when the same physical object appears across multiple views. Without this skill, models frequently double-count objects or fail to establish spatial relations that span views. The CVSR’s overlap reward (R_{overlap}) directly addresses this by incentivizing the model to track unique instances across views, learning to use shared visible objects as geometric anchors that link partial observations into a coherent global representation.

5.3 ABLATION STUDIES

To validate our design choices, we conduct a series of ablation studies. We first analyze the contribution of each component within our CVSR design, and then investigate the performance gap between reasoning from distributed ego-centric views versus a single, privileged global view. These studies provide a deeper understanding of how individual reward signals and viewpoint configurations jointly influence the emergence of robust cross-view reasoning.

Impact of CVSR Components. We ablate each component of the Cross-View Spatial Reward (CVSR) to assess its individual contribution (Table 2). Removing the answer correctness reward (R_{ans}) causes a catastrophic drop in E2W-1 accuracy from **61.0%** to 10.5%, showing that intermediate shaping signals alone cannot ensure correct final solutions. Eliminating the grounding reward (R_{ground}) reduces E2W-3(S) by over 21 points, confirming its role in aligning symbolic reasoning with precise object locations. Dropping the overlap reward (R_{overlap}) weakens counting and relational

Table 4: **Left:** Where2Place results. **Right:** Real-world robot evaluation.

Model	Score \uparrow	Task	RoboPoint	CoRL-7B
SpaceLLaVA Foutter et al. (2024)	11.8	Grasp blue block farthest from strawberry, place on red block	0.0	65.0
RoboPoint Yuan et al. (2024)	46.8			
Molmo-7B Deitke et al. (2025)	45.0	Pick carambola aligned with banana, place on red block	0.0	30.0
CoRL-7B	50.9			



Figure 4: Illustrative demonstrations of our model in real-world robotic manipulation tasks involving pick-and-place with cross-view spatial reasoning.

reasoning by impairing cross-view object consistency. Finally, the format reward (R_{format}) provides smaller but meaningful gains by enforcing structured outputs and stabilizing optimization. Together these results show that only the full CVSR, balancing correctness, grounding, consistency, and structural integrity, can robustly guide multi-view reasoning and overall embodied performance.

Multi-Views vs. Single View Reasoning. We next investigate a fundamental question: is it more effective to reason from a single global view or from multiple ego-centric views captured by distributed agents? The single-view baseline uses a global overhead camera covering the entire workspace, simulating a typical single-robot setup with full scene visibility. Table 3 shows that the multi-view configuration consistently outperforms the single view despite the latter’s complete coverage. For instance, on E2W-2(S), our multi-view approach achieves **97.0%** accuracy, significantly surpassing the single view’s 54.0%. This gap arises because a single global viewpoint suffers from perspective distortion and lacks the fine-grained geometric detail that close-range ego-centric views provide. In contrast, multiple ego-centric views, captured from diverse positions, naturally provide complementary information and broader coverage of the scene, reducing ambiguity and enabling more complete spatial reasoning.

5.4 EXTERNAL BENCHMARK: WHERE2PLACE

We further test single-image spatial grounding on **Where2Place** Yuan et al. (2024), which evaluates fine-grained point prediction from a single RGB view (Table 4, left). CoRL-7B attains 50.9 points, outperforming RoboPoint Yuan et al. (2024) (46.8) and Molmo-7B Deitke et al. (2025) (45.0). This shows that cross-view training with CVSR not only benefits multi-view reasoning but also preserves strong single-image pointing ability.

5.5 REAL-WORLD EVALUATION

We validate the effectiveness of CoRL-7B through real-world experiments. The platform comprises two Franka Research 3 arms and one Realman mobile base, each equipped with an Intel RealSense D435 RGB-D camera with calibrated extrinsics. All cameras are pre-calibrated to a shared world frame; during inference, CoRL-7B receives only the RGB images and the natural-language instruction, and predicts 2D target coordinates in a designated agent’s image. These coordinates are then lifted to 3D workspace positions using the camera’s depth channel and known intrinsics/extrinsics for downstream grasp execution. Importantly, the model itself never accesses depth or calibration data, it reasons purely from multi-view RGB inputs.

As shown in Table 4 (right), our model achieves success rates of 65% on the blue block picking task and 30% on the carambola alignment task, significantly outperforming the RoboPoint Yuan et al. (2024) baseline (0% on both tasks). These results highlight the robustness of our method in handling visual ambiguity, such as occlusions and distractors with similar colors. In particular, CoRL maintains stable predictions under viewpoint shifts, depth noise, and partial occlusions, reflecting its ability to integrate heterogeneous multi-agent observations and preserve spatial consistency in real deployments.

A key challenge in the real-world setting is bridging the sim-to-real gap. Real-world scenes introduce lighting variations, reflective surfaces, and sensor noise absent from simulation. We observe that the primary failure mode is not incorrect spatial reasoning but imprecise coordinate prediction: the model correctly identifies the target object and its approximate region, yet the predicted point occasionally falls on the object boundary. This suggests that tighter grounding supervision and resolution-aware coordinate regression are promising directions. Qualitative rollouts in Figure 4 further illustrate successful cross-view reasoning. Notably, in the blue block task, the target is partially occluded in one agent’s view but fully visible from another; CoRL leverages both perspectives to resolve the ambiguity and produce a consistent prediction.

5.6 DISCUSSION

Our comprehensive experiments convey a clear message: while model scale and pretraining provide a foundation, they are insufficient for mastering the complexities of collaborative embodied reasoning. The success of our SFT→RL pipeline highlights a crucial insight: robust spatial intelligence emerges from a structured curriculum that first bootstraps foundational, in-domain knowledge via SFT, and then refines nuanced collaborative behaviors through targeted reward shaping via CVSR. The reinforcement learning stage proves essential for teaching the model not just *what* the right answer is, but *how* to systematically derive it by grounding its reasoning in visual evidence and maintaining cross-view consistency. This is further evidenced by the RL-ZERO baseline, which attempts RL from scratch and performs poorly, demonstrating that without the structured initialization from SFT, the reward landscape is too sparse for effective policy learning. Furthermore, the ablation on input modality (Table 3) reveals a non-obvious trade-off between information density and contextual breadth. Under fixed computational budgets, multiple high-resolution local views prove more valuable than a single coarse global one, because close-range ego-centric views provide rich, complementary geometric detail that a single overhead camera, despite full workspace coverage, cannot capture due to perspective distortion. This suggests that future multi-robot systems should prioritize distributed sensing over monolithic viewpoints.

6 CONCLUSION

We introduced **CoRL**, a two-stage SFT→RL framework that equips Vision Language Models with collaborative spatial reasoning abilities from distributed ego-centric views. At the core is the Cross-View Spatial Reward (CVSR), which provides structured signals for multi-view fusion, cross-view consistency, and fine-grained grounding. Together with **E2W-Bench**, our work offers a unified testbed and methodology for studying collaborative perception in multi-agent embodied settings.

Extensive experiments demonstrate that CoRL consistently outperforms strong proprietary and open-source baselines. Ablation studies confirm that each CVSR component plays a complementary role, and that distributed ego-centric views consistently surpass a single global overhead view, validating that multi-agent perception, when properly fused through compositional reasoning, yields richer spatial understanding than any single privileged viewpoint. CoRL further generalizes to Where2Place and to real-world robotic manipulation. As embodied AI moves toward multi-robot deployments, we hope E2W-Bench and CoRL serve as a foundation for future research.

ETHICS STATEMENT

This work makes use of the publicly available Ego4D Grauman et al. (2022) dataset and the ManiSkill3 simulation platform Tao et al. (2024). The dataset was collected and released in accordance with ethical research practices, and all experiments conducted in simulation do not involve human or

animal subjects. Our study focuses on improving the capabilities of vision-language models, and we do not foresee any direct ethical concerns, including issues of privacy, safety, or fairness. We believe the potential benefits of advancing embodied AI research outweigh the minimal risks, and no conflicts of interest or ethical violations are associated with this work.

REPRODUCIBILITY STATEMENT

We have taken extensive measures to ensure the reproducibility of our work. All code related to data preprocessing, model training, and evaluation is released at CoRL, and the trained models will be hosted on Hugging Face for public access. The processed data used in our experiments will also be made available to facilitate replication. Furthermore, detailed experimental settings, including hyperparameters, training schedules, and environment configurations, are documented in the appendix and supplementary materials.

REFERENCES

- Shuai Bai, Keqin Chen, Xuejing Liu, Jialin Wang, Wenbin Ge, Siboz Song, Kai Dang, Peng Wang, Shijie Wang, Jun Tang, et al. Qwen2. 5-vl technical report. *arXiv preprint arXiv:2502.13923*, 2025.
- Xiaohu Bo, Zeyu Zhang, Quanyu Dai, Xueyang Feng, Lei Wang, Rui Li, Xu Chen, and Ji-Rong Wen. Reflective multi-agent collaboration based on large language models. *Advances in Neural Information Processing Systems*, 37:138595–138631, 2024.
- Shaofei Cai, Zhancun Mu, Anji Liu, and Yitao Liang. Rocket-2: Steering visuomotor policy via cross-view goal alignment, 2025.
- Mathilde Caron, Hugo Touvron, Ishan Misra, Hervé Jégou, Julien Mairal, Piotr Bojanowski, and Armand Joulin. Emerging properties in self-supervised vision transformers. In *Proceedings of the IEEE/CVF international conference on computer vision*, pp. 9650–9660, 2021.
- Yang Chen, Yufan Shen, Wenxuan Huang, Sheng Zhou, Qunshu Lin, Xinyu Cai, Zhi Yu, Jiajun Bu, Botian Shi, and Yu Qiao. Learning only with images: Visual reinforcement learning with reasoning, rendering, and visual feedback. *arXiv preprint arXiv:2507.20766*, 2025.
- Gheorghe Comanici, Eric Bieber, Mike Schaekermann, Ice Pasupat, Noveen Sachdeva, Inderjit Dhillon, Marcel Blistein, Ori Ram, Dan Zhang, Evan Rosen, et al. Gemini 2.5: Pushing the frontier with advanced reasoning, multimodality, long context, and next generation agentic capabilities. *arXiv preprint arXiv:2507.06261*, 2025.
- Matt Deitke, Christopher Clark, Sangho Lee, Rohun Tripathi, Yue Yang, Jae Sung Park, Mohammadreza Salehi, Niklas Muennighoff, Kyle Lo, Luca Soldaini, et al. Molmo and pixmo: Open weights and open data for state-of-the-art vision-language models. In *Proceedings of the Computer Vision and Pattern Recognition Conference*, pp. 91–104, 2025.
- Abhimanyu Dubey, Abhinav Jauhri, Abhinav Pandey, Abhishek Kadian, Ahmad Al-Dahle, Aiesha Letman, Akhil Mathur, Alan Schelten, Amy Yang, Angela Fan, et al. The llama 3 herd of models. *arXiv e-prints*, pp. arXiv–2407, 2024.
- Hao-Shu Fang, Chenxi Wang, Hongjie Fang, Minghao Gou, Jirong Liu, Hengxu Yan, Wenhui Liu, Yichen Xie, and Cewu Lu. Anygrasp: Robust and efficient grasp perception in spatial and temporal domains. *IEEE Transactions on Robotics*, 39(5):3929–3945, 2023.
- Jodi Forlizzi and Carl DiSalvo. Service robots in the domestic environment: a study of the roomba vacuum in the home. In *Proceedings of the 1st ACM SIGCHI/SIGART Conference on Human-Robot Interaction*, HRI '06, pp. 258–265. Association for Computing Machinery, 2006. doi: 10.1145/1121241.1121286.
- Matthew Foutter, Daniele Gammelli, Justin Kruger, Ethan Foss, Praneet Bhoj, Tommaso Guffanti, Simone D’Amico, and Marco Pavone. Space-llava: a vision-language model adapted to extraterrestrial applications. *arXiv preprint arXiv:2408.05924*, 2024.

- Jiahui Gao, Renjie Pi, Jipeng Zhang, Jiacheng Ye, Wanjun Zhong, Yufei Wang, Lanqing Hong, Jianhua Han, Hang Xu, Zhenguo Li, et al. G-llava: Solving geometric problem with multi-modal large language model. *arXiv preprint arXiv:2312.11370*, 2023.
- Kristen Grauman, Andrew Westbury, Eugene Byrne, Zachary Chavis, Antonino Furnari, Rohit Girdhar, Jackson Hamburger, Hao Jiang, Miao Liu, Xingyu Liu, et al. Ego4d: Around the world in 3,000 hours of egocentric video. In *Proceedings of the IEEE/CVF conference on computer vision and pattern recognition*, pp. 18995–19012, 2022.
- Daya Guo, Dejian Yang, Haowei Zhang, Junxiao Song, Ruoyu Zhang, Runxin Xu, Qihao Zhu, Shirong Ma, Peiyi Wang, Xiao Bi, et al. Deepseek-r1: Incentivizing reasoning capability in llms via reinforcement learning. *arXiv preprint arXiv:2501.12948*, 2025.
- Xudong Guo, Kaixuan Huang, Jiale Liu, Wenhui Fan, Natalia Vélez, Qingyun Wu, Huazheng Wang, Thomas L Griffiths, and Mengdi Wang. Embodied llm agents learn to cooperate in organized teams. *arXiv preprint arXiv:2403.12482*, 2024.
- Yingdong Hu, Fanqi Lin, Tong Zhang, Li Yi, and Yang Gao. Look before you leap: Unveiling the power of gpt-4v in robotic vision-language planning. *arXiv preprint arXiv:2311.17842*, 2023.
- Yuheng Ji, Huajie Tan, Jiayu Shi, Xiaoshuai Hao, Yuan Zhang, Hengyuan Zhang, Pengwei Wang, Mengdi Zhao, Yao Mu, Pengju An, et al. Robobrain: A unified brain model for robotic manipulation from abstract to concrete. *arXiv preprint arXiv:2502.21257*, 2025.
- Haobin Jiang and Zongqing Lu. Visual grounding for object-level generalization in reinforcement learning. In *European Conference on Computer Vision*, pp. 55–72. Springer, 2024.
- Li Kang, Xiufeng Song, Heng Zhou, Yiran Qin, Jie Yang, Xiaohong Liu, Philip Torr, Lei Bai, and Zhenfei Yin. Viki-r: Coordinating embodied multi-agent cooperation via reinforcement learning. *arXiv preprint arXiv:2506.09049*, 2025.
- Li Kang, Heng Zhou, Xiufeng Song, Rui Li, Bruno NY Chen, Ziyi Wang, Ximeng Meng, Stone Tao, Yiran Qin, Xiaohong Liu, et al. Advances and innovations in the multi-agent robotic system (mars) challenge. *arXiv preprint arXiv:2601.18733*, 2026.
- Jiaqi Liu, Chengkai Xu, Peng Hang, Jian Sun, Mingyu Ding, Wei Zhan, and Masayoshi Tomizuka. Language-driven policy distillation for cooperative driving in multi-agent reinforcement learning. *IEEE Robotics and Automation Letters*, 2025a.
- Si Liu, Chen Gao, Yuan Chen, Xingyu Peng, Xianghao Kong, Kun Wang, Runsheng Xu, Wentao Jiang, Hao Xiang, Jiaqi Ma, and Miao Wang. Towards vehicle-to-everything autonomous driving: A survey on collaborative perception, 2023.
- Xiangyan Liu, Jinjie Ni, Zijian Wu, Chao Du, Longxu Dou, Haonan Wang, Tianyu Pang, and Michael Qizhe Shieh. Noisyrollout: Reinforcing visual reasoning with data augmentation. *arXiv preprint arXiv:2504.13055*, 2025b.
- Ziyu Liu, Zeyi Sun, Yuhang Zang, Xiaoyi Dong, Yuhang Cao, Haodong Duan, Dahua Lin, and Jiaqi Wang. Visual-rft: Visual reinforcement fine-tuning. *arXiv preprint arXiv:2503.01785*, 2025c.
- Soroush Nasiriany, Abhiram Maddukuri, Lance Zhang, Adeet Parikh, Aaron Lo, Abhishek Joshi, Ajay Mandlekar, and Yuke Zhu. Robocasa: Large-scale simulation of everyday tasks for generalist robots. *arXiv preprint arXiv:2406.02523*, 2024.
- Kazuma Obata, Tatsuya Aoki, Takato Horii, Tadahiro Taniguchi, and Takayuki Nagai. Lip-llm: Integrating linear programming and dependency graph with large language models for multi-robot task planning. *IEEE Robotics and Automation Letters*, 2024.
- OpenAI. Introducing gpt-5, August 2025.
- Yiran Qin, Li Kang, Xiufeng Song, Zhenfei Yin, Xiaohong Liu, Xihui Liu, Ruimao Zhang, and Lei Bai. Robofactory: Exploring embodied agent collaboration with compositional constraints. *arXiv preprint arXiv:2503.16408*, 2025a.

- Yiran Qin, Jiahua Ma, Li Kang, Wenzhan Li, Xiufeng Song, Heng Zhou, Jiwen Yu, Zhenfei Yin, Xihui Liu, Philip Torr, et al. Building scalable real-world robot data generation via compositional simulation. *arXiv preprint*, 2025b.
- Yiran Qin, Zhemeng Zhang, Heng Zhou, Li Kang, Bruno NY Chen, Ximeng Meng, Xiufeng Song, Jiahua Ma, Zhenfei Yin, Xiaohong Liu, et al. Robomonster: Compositional generalization of heterogeneous multi-end effector embodied agents. *arXiv preprint*, 2025c.
- Nikhila Ravi, Valentin Gabeur, Yuan-Ting Hu, Ronghang Hu, Chaitanya Ryali, Tengyu Ma, Haitham Khedr, Roman Rädle, Chloe Rolland, Laura Gustafson, et al. Sam 2: Segment anything in images and videos. *arXiv preprint arXiv:2408.00714*, 2024.
- Gabriel Sarch, Snigdha Saha, Naitik Khandelwal, Ayush Jain, Michael J Tarr, Aviral Kumar, and Katerina Fragkiadaki. Grounded reinforcement learning for visual reasoning. *arXiv preprint arXiv:2505.23678*, 2025.
- ByteDance Seed. Seed 1.6, 2025. URL https://seed.bytedance.com/en/seed1_6.
- Yongqi Shen et al. VLM-R1: A stable and generalizable R1-style large vision-language model. *arXiv preprint arXiv:2504.xxxxx*, 2025.
- Wenhao Shi, Zhiqiang Hu, Yi Bin, Junhua Liu, Yang Yang, See-Kiong Ng, Lidong Bing, and Roy Ka-Wei Lee. Math-llava: Bootstrapping mathematical reasoning for multimodal large language models. *arXiv preprint arXiv:2406.17294*, 2024.
- Huajie Tan, Yuheng Ji, Xiaoshuai Hao, Minglan Lin, Pengwei Wang, Zhongyuan Wang, and Shanghang Zhang. Reason-rft: Reinforcement fine-tuning for visual reasoning. *arXiv preprint arXiv:2503.20752*, 2025.
- Stone Tao, Fanbo Xiang, Arth Shukla, Yuzhe Qin, Xander Hinrichsen, Xiaodi Yuan, Chen Bao, Xinsong Lin, Yulin Liu, Tse-kai Chan, et al. Maniskill3: Gpu parallelized robotics simulation and rendering for generalizable embodied ai. *arXiv preprint arXiv:2410.00425*, 2024.
- V Team, Wenyi Hong, Wenmeng Yu, Xiaotao Gu, Guo Wang, Guobing Gan, Haomiao Tang, Jiale Cheng, Ji Qi, Junhui Ji, Lihang Pan, Shuaiqi Duan, Weihang Wang, Yan Wang, Yean Cheng, Zehai He, Zhe Su, Zhen Yang, Ziyang Pan, Aohan Zeng, Baoxu Wang, Bin Chen, Boyan Shi, Changyu Pang, Chenhui Zhang, Da Yin, Fan Yang, Guoqing Chen, Jiazheng Xu, Jiale Zhu, Jiali Chen, Jing Chen, Jinhao Chen, Jinghao Lin, Jinjiang Wang, Junjie Chen, Leqi Lei, Letian Gong, Leyi Pan, Mingdao Liu, Mingde Xu, Mingzhi Zhang, Qinkai Zheng, Sheng Yang, Shi Zhong, Shiyu Huang, Shuyuan Zhao, Siyan Xue, Shangqin Tu, Shengbiao Meng, Tianshu Zhang, Tianwei Luo, Tianxiang Hao, Tianyu Tong, Wenkai Li, Wei Jia, Xiao Liu, Xiaohan Zhang, Xin Lyu, Xinyue Fan, Xuancheng Huang, Yanling Wang, Yadong Xue, Yanfeng Wang, Yanzi Wang, Yifan An, Yifan Du, Yiming Shi, Yiheng Huang, Yilin Niu, Yuan Wang, Yuanchang Yue, Yuchen Li, Yutao Zhang, Yuting Wang, Yu Wang, Yuxuan Zhang, Zhao Xue, Zhenyu Hou, Zhengxiao Du, Zihan Wang, Peng Zhang, Debing Liu, Bin Xu, Juanzi Li, Minlie Huang, Yuxiao Dong, and Jie Tang. Glm-4.5v and glm-4.1v-thinking: Towards versatile multimodal reasoning with scalable reinforcement learning, 2025.
- Weizheng Wang, Ike Obi, and Byung-Cheol Min. Multi-agent llm actor-critic framework for social robot navigation. *arXiv preprint arXiv:2503.09758*, 2025a.
- Yongdong Wang, Runze Xiao, Jun Younes Louhi Kasahara, Ryosuke Yajima, Keiji Nagatani, Atsushi Yamashita, and Hajime Asama. Dart-llm: Dependency-aware multi-robot task decomposition and execution using large language models. *arXiv preprint arXiv:2411.09022*, 2024.
- Yujin Wang, Quanfeng Liu, Zhengxin Jiang, Tianyi Wang, Junfeng Jiao, Hongqing Chu, Bingzhao Gao, and Hong Chen. Rad: Retrieval-augmented decision-making of meta-actions with vision-language models in autonomous driving. *arXiv preprint arXiv:2503.13861*, 2025b.
- Jason Wei, Xuezhi Wang, Dale Schuurmans, Maarten Bosma, Fei Xia, Ed Chi, Quoc V Le, Denny Zhou, et al. Chain-of-thought prompting elicits reasoning in large language models. *Advances in neural information processing systems*, 35:24824–24837, 2022.

- Guowei Xu, Peng Jin, Li Hao, Yibing Song, Lichao Sun, and Li Yuan. Llava-cot: Let vision language models reason step-by-step, 2024. URL <https://arxiv.org/abs/2411.10440>, 2024.
- An Yang, Anfeng Li, Baosong Yang, Beichen Zhang, Binyuan Hui, Bo Zheng, Bowen Yu, Chang Gao, Chengen Huang, Chenxu Lv, et al. Qwen3 technical report. *arXiv preprint arXiv:2505.09388*, 2025.
- Jiafei Ye et al. VLA-R1: Enhancing reasoning in vision-language-action models. *arXiv preprint arXiv:2505.xxxxx*, 2025.
- Baiqiao Yin, Qineng Wang, Pingyue Zhang, Jianshu Zhang, Kangrui Wang, Zihan Wang, Jieyu Zhang, Keshigeyan Chandrasegaran, Han Liu, Ranjay Krishna, Saining Xie, Manling Li, Jiajun Wu, and Li Fei-Fei. Spatial mental modeling from limited views, 2025. URL <https://arxiv.org/abs/2506.21458>.
- Wentao Yuan, Jiafei Duan, Valts Blukis, Wilbert Pumacay, Ranjay Krishna, Adithyavairavan Murali, Arsalan Mousavian, and Dieter Fox. Robopoint: A vision-language model for spatial affordance prediction for robotics. *arXiv preprint arXiv:2406.10721*, 2024.
- Guibin Zhang, Hejia Geng, Xiaohang Yu, Zhenfei Yin, Zaibin Zhang, Zelin Tan, Heng Zhou, Zhongzhi Li, Xiangyuan Xue, Yijiang Li, et al. The landscape of agentic reinforcement learning for llms: A survey. *TMLR*, 2025.
- Hongxin Zhang, Weihua Du, Jiaming Shan, Qinhong Zhou, Yilun Du, Joshua B Tenenbaum, Tianmin Shu, and Chuang Gan. Building cooperative embodied agents modularly with large language models. *arXiv preprint arXiv:2307.02485*, 2023a.
- Hongxin Zhang, Zeyuan Wang, Qiushi Lyu, Zheyuan Zhang, Sunli Chen, Tianmin Shu, Behzad Dariush, Kwonjoon Lee, Yilun Du, and Chuang Gan. Combo: compositional world models for embodied multi-agent cooperation. *arXiv preprint arXiv:2404.10775*, 2024a.
- Renrui Zhang, Xinyu Wei, Dongzhi Jiang, Ziyu Guo, Shicheng Li, Yichi Zhang, Chengzhuo Tong, Jiaming Liu, Aojun Zhou, Bin Wei, et al. Mathematical visual instruction tuning with an automatic data engine. *arXiv preprint arXiv:2407.08739*, 2024b.
- Ruohong Zhang, Bowen Zhang, Yanghao Li, Haotian Zhang, Zhiqing Sun, Zhe Gan, Yinfei Yang, Ruoming Pang, and Yiming Yang. Improve vision language model chain-of-thought reasoning. *arXiv preprint arXiv:2410.16198*, 2024c.
- Youcai Zhang, Xinyu Huang, Jinyu Ma, Zhaoyang Li, Zhaochuan Luo, Yanchun Xie, Yuzhuo Qin, Tong Luo, Yaqian Li, Shilong Liu, et al. Recognize anything: A strong image tagging model. *arXiv preprint arXiv:2306.03514*, 2023b.
- Enshen Zhou, Jingkun An, Cheng Chi, Yi Han, Shanyu Rong, Chi Zhang, Pengwei Wang, Zhongyuan Wang, Tiejun Huang, Lu Sheng, et al. Roborefer: Towards spatial referring with reasoning in vision-language models for robotics. *arXiv preprint arXiv:2506.04308*, 2025.
- Xuhui Zhou, Hao Zhu, Leena Mathur, Ruohong Zhang, Haofei Yu, Zhengyang Qi, Louis-Philippe Morency, Yonatan Bisk, Daniel Fried, Graham Neubig, et al. Sotopia: Interactive evaluation for social intelligence in language agents. *arXiv preprint arXiv:2310.11667*, 2023.
- Yifeng Zhu, Abhishek Joshi, Peter Stone, and Yuke Zhu. Viola: Imitation learning for vision-based manipulation with object proposal priors. *arXiv preprint arXiv:2210.11339*, 2022. doi: 10.48550/arXiv.2210.11339.
- Yuke Zhu, Roozbeh Mottaghi, Eric Kolve, Joseph J Lim, Abhinav Gupta, Li Fei-Fei, and Ali Farhadi. Target-driven visual navigation in indoor scenes using deep reinforcement learning. In *2017 IEEE International Conference on Robotics and Automation (ICRA)*, pp. 3357–3364. IEEE, 2017.

Supplementary Material

A LIMITATIONS AND FUTURE WORK

Despite the promising results, several limitations point to directions for future research. First, our framework operates on static, synchronized snapshots from all agents; in practice, distributed robots may capture observations at different times or with varying latencies. Extending CoRL to handle asynchronous sensing and temporal reasoning over video streams is an important next step. Second, the current architecture adopts a centralized design in which a single VLM processes all views jointly. While effective for a small number of agents, this imposes communication overhead and a single point of failure; its scalability to scenarios involving a large fleet of agents warrants further investigation into more efficient, perhaps hierarchical or message-passing-based, fusion strategies. Third, our benchmark does not yet address dynamic scenes with moving objects or agents, which would require tracking and re-identification across time as well as views. Fourth, the current coordinate prediction operates in 2D image space; incorporating depth information for full 3D spatial grounding would broaden applicability to tasks requiring precise manipulation in three dimensions. Finally, while our data covers 50+ object categories, the long-tail distribution of real-world environments suggests that further work on domain-invariant representations and open-vocabulary grounding could strengthen generalization.

This work opens several exciting directions. Future research could explore decentralized architectures where agents learn to communicate condensed, relevant information rather than sharing raw visual data. Another compelling avenue is the extension of CoRL to long-horizon, multi-step collaborative tasks, moving beyond single-step perception and grasping towards complex manipulation and navigation. Ultimately, we believe these directions offer promising avenues for advancing VLM-driven embodied collaboration and the construction of coherent world models from distributed views.

B OTHER RELATED WORK AND NOVELTY

Recent work has begun to explore cross-view reasoning, yet these efforts remain fundamentally different from our problem setting. ROCKET-2 Cai et al. (2025) focuses on cross-view goal alignment for a *single* visuomotor agent, where human and agent viewpoints differ; its approach introduces auxiliary losses (e.g., visibility and consistency losses) to improve policy cloning, but does not address the integration of multiple ego-centric observations or collaborative inference across agents. MindCube Yin et al. (2025) instead evaluates whether VLMs can form *spatial mental models* of static scenes from a few partial snapshots, emphasizing cognitive mapping and perspective-taking in a non-embodied setting without action generation or multi-agent coordination. Other concurrent works Yuan et al. (2024); Foutter et al. (2024); Deitke et al. (2025) investigate single-image spatial grounding or 3D-aware perception, but assume a single camera and do not consider distributed viewpoint fusion or embodied multi-view decision-making.

In contrast, our work introduces a **new embodied multi-agent setting** in which multiple robots simultaneously collect heterogeneous ego-centric views, and a central VLM must perform *collaborative spatial reasoning* by fusing these distributed observations. This setting captures challenges—such as complementary visibility, cross-view ambiguity, and viewpoint-dependent grounding—that do not arise in prior single-agent or single-view formulations. To support systematic study of this problem, we present **E2W-Bench**, the first benchmark designed for world-centric reasoning from distributed embodied viewpoints across counting, relational QA, and view-specific grasp prediction. Moreover, to effectively solve this challenging setting, we propose **CoRL**, a two-stage SFT→RL framework equipped with the **Cross-View Spatial Reward (CVSR)**, which explicitly shapes multi-view grounding, overlap reasoning, and final answer correctness. Together, E2W-Bench and CoRL define a principled paradigm for multi-agent, multi-view spatial reasoning in embodied environments—going beyond prior cross-view or spatial QA works and establishing a novel direction for collaborative embodied AI.

C PROBLEM SETUP & NOTATION

In this section, we formally define the problem setup and introduce the notation used throughout the paper. We focus on the collaborative spatial reasoning task within multi-agent embodied systems, where multiple agents contribute to the construction of a shared understanding of a scene from partial observations.

C.1 PROBLEM SETUP

We consider a system of N agents, each represented by an individual agent a_i for $i \in \{1, \dots, N\}$. Each agent a_i perceives the environment through a limited, ego-centric viewpoint, denoted by \mathcal{V}_i . The environment \mathcal{E} is a spatial scene consisting of various objects, denoted by $\mathcal{O} = \{o_1, o_2, \dots, o_M\}$, where M is the total number of objects in the scene. Each object o_j has associated properties, such as position, orientation, and object class, which we denote by $\mathbf{p}_j = (x_j, y_j, z_j)$, $\mathbf{r}_j = (\theta_j, \phi_j)$, and c_j respectively.

The goal of the system is to enable the agents to collaboratively reason about the scene, including the localization of objects, the spatial relationships between objects, and the execution of spatially grounded actions. To achieve this, each agent a_i shares its ego-centric observation \mathcal{V}_i with a central Vision–Language Model (VLM), which integrates the individual observations to build a global understanding of the scene.

The task is formalized as a spatial reasoning problem, where the agents must complete a set of spatial tasks, such as object localization, relationship inference, and action planning, by collectively reasoning over their partial observations. Specifically, we aim to develop a system where the agents’ observations are integrated effectively to:

- Localize objects across different viewpoints.
- Infer spatial relationships between objects.
- Plan and execute actions based on a shared understanding of the scene.

C.2 NOTATION

We define the following notation used in this paper:

- \mathcal{A} : Set of agents, where $\mathcal{A} = \{a_1, a_2, \dots, a_N\}$, and each agent a_i has its own ego-centric observation \mathcal{V}_i .
- \mathcal{O} : Set of objects in the scene, $\mathcal{O} = \{o_1, o_2, \dots, o_M\}$.
- \mathcal{V}_i : Ego-centric observation of agent a_i , containing visual and linguistic information relevant to the agent’s current view of the scene.
- \mathbf{p}_j : Position of object o_j , represented as a 3D vector (x_j, y_j, z_j) .
- \mathbf{r}_j : Orientation of object o_j , represented by angles (θ_j, ϕ_j) .
- c_j : Class of object o_j , which can be one of a predefined set of object categories.
- Q : A natural-language query describing the task to be performed.
- π_θ : The central VLM policy parameterized by θ , which integrates all ego-centric observations and the query to produce a prediction \hat{y} .
- \hat{y} : The model prediction, either a textual response (for counting and relational reasoning) or a pair of image-plane coordinates (for grasping).
- R : The reward function evaluating the quality of \hat{y} against the ground-truth label y .

C.3 TASK DEFINITION

We define the collaborative spatial reasoning task as a sequential decision-making process where each agent must select an action from the set \mathcal{A}_i based on its perception \mathcal{V}_i and the shared scene information. The goal is to maximize the collective performance across all agents, measured by a

global reward function that takes into account the accuracy of object localization, the correct inference of spatial relationships, and the successful execution of grounded actions.

The multi-agent system operates under the assumption of partial observability, meaning that each agent only has access to a limited subset of the scene and must rely on the collaboration of other agents to complete the task. The system must overcome the challenges of occlusions, incomplete observations, and ambiguous spatial relationships to successfully execute actions in a dynamic environment.

C.4 ASSUMPTIONS

The following assumptions are made for the proposed problem setup:

- Each agent has access to an ego-centric camera or sensor that provides partial observations of the scene.
- Agents can communicate with each other to share observations and jointly reason about the spatial layout of the environment.
- The central VLM has access to all agent observations and coordinates the integration of these inputs for collaborative reasoning.
- The agents' actions are executed in discrete time steps, and the environment responds to each action with a new state.

D E2W BENCHMARK DETAILS

In this section, we provide detailed information about the E2W data, which consists of both simulated and real-world data. The dataset includes over 100k simulated samples and more than 60k real-world samples. The benchmark is organized into three tasks, each with a distinct focus on collaborative spatial reasoning. Below, we describe the structure and data distribution for each task.

D.1 DATASET OVERVIEW

The E2W benchmark consists of the following components:

- **Simulated Data:** A total of over 100k samples were collected from simulations, which provide a diverse set of scenes and spatial configurations for training and evaluation.
- **Real-World Data:** Over 60k samples were gathered from real-world environments, capturing the complexity of physical spaces and sensor noise that is typical in practical scenarios.

D.2 TASK BREAKDOWN

The E2W benchmark includes three distinct tasks designed to evaluate different aspects of collaborative spatial reasoning:

- **Task 1 (Counting Task):** This task focuses on the ability of the agents to count the number of objects within a scene. It is solely based on the simulated data, as real-world data for this task was not available.
- **Task 2 (Location Reasoning):** This task evaluates the agents' ability to infer spatial relations among objects that never co-occur in a single view, requiring cross-view reasoning to answer correctly in natural language. Both simulated and real-world data are used, with the real-world data providing additional complexity due to sensor noise and occlusions.
- **Task 3 (Grasping):** In this task, agents are required to translate a language command involving spatial relations into precise 2D coordinates within a specific agent's viewpoint, linking compositional reasoning to downstream robotic manipulation. Like Task 2, this task uses both simulated and real-world data.

D.3 DATASET SPLITS

For each task, we carefully curated the dataset as follows:

- **Test Set:** For each task, we selected 200 high-quality samples to form the test set, ensuring that it covers a wide range of challenging scenarios.
- **Cold-Start Set (COT):** We prepared a cold-start set consisting of 1000 samples, which is used to initialize the model before training. This set includes diverse configurations that enable the agents to begin learning without prior knowledge of the environment.
- **Training Set:** The remaining samples were used for training, with 90k samples from the simulated data contributing to the training set. The real-world data (6k samples) was integrated into the training set, but it is more sparsely used compared to the simulated data, ensuring a balance between generalizability and real-world applicability.

Task	Simulated Data	Real-World Data	Total Data
Task 1 (Counting)	30k	0	30k
Task 2 (Location Reasoning)	35k	25k	60k
Task 3 (Grasping)	35k	35k	70k

Table 5: E2W Benchmark Dataset Distribution for Each Task

D.4 DATA QUALITY AND SELECTION CRITERIA

Each task in the benchmark was carefully designed to cover a range of real-world challenges in collaborative spatial reasoning. To ensure high data quality, we followed strict selection criteria for both simulated and real-world data:

- The simulated data was generated using a variety of scene configurations, object types, and spatial relationships to create a comprehensive and diverse training set.
- For the real-world data, we selected scenarios with clear object localization, minimal occlusions, and representative spatial relationships to maximize the relevance of the data for evaluating real-world performance.
- We prioritized edge cases and challenging scenarios for the test sets, ensuring that they push the limits of the agents’ reasoning abilities and provide meaningful benchmarks for model performance.

D.5 DATA COLLECTION

Simulation Data All task data are collected in a high-fidelity simulation environment built upon RoboFactory Qin et al. (2025a) and ManiSkill3 Tao et al. (2024), following scalable compositional simulation principles Qin et al. (2025b), which provide diverse scenes like RoboCasa Nasiriany et al. (2024), articulated objects, and multi-agent configurations. We curate over 15,000 multi-agent samples across dozens of spatial layouts, each scene populated with a rich combination of manipulable objects under varied configurations. For every instance, synchronized global and egocentric camera views are recorded to support collaborative reasoning. Ground-truth annotations, including object counts, spatial relations, and manipulation-relevant attributes, are automatically derived from simulator metadata and physics engines, followed by human verification to ensure semantic consistency. This pipeline ensures that the resulting dataset captures the complementary demands of multi-view spatial reasoning, ranging from global aggregation to relational understanding and action grounding.

Real-World Data To complement simulation environments with naturalistic observations, we leverage the Ego4D dataset Grauman et al. (2022), a massive-scale egocentric video corpus spanning 74 worldwide locations across 9 countries, with over 3,670 hours of daily-life recordings. Ego4D offers unconstrained visual contexts that reflect the challenges of embodied perception in realistic human environments. For data preparation, we first extract video frames at uniform intervals to obtain

temporally diverse samples. We then apply strong vision backbones, including Region Attention Masking (RAM) Zhang et al. (2023b) for object-level proposals and DINO Caron et al. (2021) for robust feature alignment, to automatically annotate object instances and spatial relations. Through this pipeline, we curate two subsets aligned with our benchmarks: **E2W-2-Real** (relational reasoning) and **E2W-3-Real** (grasping-oriented perception), each containing approximately 30k samples, yielding a total of 60k real-world instances. This large-scale collection bridges the gap between simulation and reality by introducing natural visual noise, diverse object appearances, and unconstrained scene dynamics.

E METHOD DETAILS (CoRL)

In this section, we provide a detailed description of the proposed Collaborative Spatial Reasoning Reinforcement Learning (CoRL) framework. We outline the training objective, pipeline, and key components of the approach, which enable effective multi-agent collaborative spatial reasoning.

E.1 TRAINING OBJECTIVE & PIPELINE

The training objective for our proposed CoRL framework is designed to guide the agents towards improving their collaborative spatial reasoning capabilities. The main goal is to maximize the agents’ ability to effectively integrate their partial, ego-centric observations and reason about the global spatial scene. To achieve this, we combine reinforcement learning (RL) with a novel Cross-View Spatial Reward (CVSR) function, which shapes the learning process by encouraging the agents to perform tasks that require accurate spatial localization, object relationships inference, and collaborative decision-making.

E.1.1 REINFORCEMENT LEARNING SETUP

We adopt a reinforcement learning setup, where each agent interacts with its environment and receives feedback in the form of a reward signal. The environment consists of a spatial scene with multiple agents, and each agent’s objective is to complete a set of spatial reasoning tasks, such as object localization and relationship inference.

Each agent a_i receives a partial observation \mathcal{V}_i of the scene, which includes both visual and linguistic information. Based on this observation, the agent selects an action $a_i(t)$ from a predefined set of actions y_i . The agent’s action affects the state of the environment, and the environment responds by providing a new state and a corresponding reward $r_i(t)$, which is calculated by the Cross-View Spatial Reward (CVSR) function.

The overall training objective is to maximize the expected cumulative reward for each agent:

$$J(\theta) = \mathbb{E} \left[\sum_{t=0}^T \gamma^t r_i(t) \right]$$

where T is the total number of time steps in the task, γ is the discount factor, and $r_i(t)$ is the reward signal at time step t .

E.2 HYPERPARAMETERS FOR REWARD AND CVSR

In our CoRL framework, we define several hyperparameters for the reward function and Cross-View Spatial Reward (CVSR) that guide the agents’ training process. These weights are carefully tuned to balance the different components of the task, ensuring that the agents effectively learn to perform spatial reasoning across multiple agents and viewpoints.

E.2.1 CVSR COMPONENTS WEIGHTS

The Cross-View Spatial Reward (CVSR) function is designed to guide agents in overcoming challenges like occlusions, incomplete observations, and the need for integration across multiple viewpoints. The CVSR reward is composed of three components:

$$R_{CVSR} = w_{ground} R_{ground} + w_{overlap} R_{overlap} + w_{ans} R_{ans},$$

where the components are:

- $w_{ans} = 0.7$: The weight for Answering (the ability to correctly complete the task based on spatial reasoning). This is the most important component, as it directly measures the success of the agent in solving the task.
- $w_{ground} = 0.1$: The weight for Localization (the ability to accurately localize objects in the scene). While important, this is a lower priority in comparison to answering tasks, as it is a fundamental skill that supports other reasoning tasks.
- $w_{overlap} = 0.2$: The weight for Fusion of Observations (the integration of ego-centric views). This component ensures the agents combine their partial observations to build a more complete understanding of the environment, and is essential for collaborative spatial reasoning.

These weights are chosen to emphasize the importance of answering correctly, while still ensuring that localization and fusion of observations are effectively learned.

E.2.2 TRAINING PIPELINE

The training pipeline for the CoRL framework follows a two-phase process: Supervised Fine-Tuning (SFT) followed by Reinforcement Learning (RL). The pipeline is as follows:

- **Phase 1: Supervised Fine-Tuning (SFT)**: In this phase, the agents are first pre-trained using supervised learning. The goal is to initialize the model with basic spatial reasoning skills, using labeled data from the training set. The agents learn to perform tasks such as object localization and relationship inference based on ground truth labels.
- **Phase 2: Reinforcement Learning (RL)**: After the initial fine-tuning, the agents enter the RL phase, where they learn to improve their performance through interactions with the environment. The CVSR function is used to guide the agents’ actions and refine their spatial reasoning capabilities. During this phase, agents iteratively adjust their policies to maximize the cumulative reward.

The overall training process is summarized in Algorithm 1.

Algorithm 1 CoRL Training Pipeline

- 1: **Input:** Pre-trained VLM parameters θ , training dataset \mathcal{D} , CVSR weights $w_{ground}, w_{overlap}, w_{ans}$, group size G
 - 2: **Phase 1: Supervised Fine-Tuning (SFT)**
 - 3: **for** each CoT-annotated sample $(x, q, r, a) \in \mathcal{D}$ **do**
 - 4: Minimize \mathcal{L}_{SFT} (Eq. 3 in the main paper) via next-token prediction on $y = [r, a]$
 - 5: **end for**
 - 6: Obtain SFT-initialized policy $\pi_0 \leftarrow \pi_\theta$
 - 7: **Phase 2: Reinforcement Learning (GRPO)**
 - 8: **for** each training step **do**
 - 9: Sample input $u = (\{I_i\}_{i=1}^N, Q)$ from \mathcal{D}
 - 10: Generate G candidate responses $\{y_j\}_{j=1}^G$ from π_θ
 - 11: Score each y_j with reward $R_j = \lambda_1 R_{format} + \lambda_2 R_{CVSR}$
 - 12: Compute group-relative advantages $\mathcal{A}_j = (R_j - \bar{R})/\sigma_R$
 - 13: Update θ by maximizing $\mathcal{J}(\theta)$ (Eq. 7 in the main paper)
 - 14: **end for**
-

F REAL-WORLD ROBOTIC EVALUATION

We implement our real-world evaluation on manipulation platform equipped with two Franka Research 3 arms and a Realman mobile base. Each arm is paired with an Intel RealSense D435 RGB-D camera beside the robotic arm, and all cameras are extrinsically calibrated to a common base frame.

In the open-loop execution mode, CoRL-7B processes synchronized multi-view RGB images and predicts the 2D target location for the instructed action. The 2D coordinates are first fed into SAM2 Ravi et al. (2024) to generate a segmentation mask, which filters the target object’s point cloud from the RGB-D stream of the D435. The extracted point cloud is then passed to AnyGrasp Fang et al. (2023), which predicts a feasible grasp pose in the camera coordinate frame. Using the pre-calibrated camera extrinsics, the grasp pose is transformed into the coordinate system of the selected robotic arm. Then, we use the Deoxys library Zhu et al. (2022) to interact with the Franka Control Interface.

For placement, CoRL-7B outputs a 2D placement location, which is converted into 3D coordinates using the depth data. This 3D point is similarly transformed into the robot’s coordinate frame, and the arm follows an open-loop trajectory to release the object at the designated position.

This setup allows us to directly connect vision–language inference with physical manipulation through SAM2-based segmentation and AnyGrasp-based grasp synthesis, without closed-loop corrections. It highlights the model’s ability to produce actionable spatial predictions from multi-view observations.

G PROMPT DESIGN AND EVALUATION PROTOCOLS

G.1 SPATIAL QA GENERATION

Dual-Image Spatial Reasoning Prompt (with Auxiliary View).

System Prompt

You are provided with two images for multi-image reasoning. The
 ↪ first image shows labeled
 objects with their bounding box coordinates: {object_labels}. The
 ↪ second image is an auxiliary
 view taken {time_interval} seconds later that may provide
 ↪ additional context.

Please generate spatial relationship questions based primarily on
 ↪ the first image, while
 having access to both images:

1. Generate 2-3 questions about the spatial relationship between
 ↪ the {obj1} and the {obj2}.
2. Base your questions on the labeled objects in the first image.
3. Use the coordinate information to understand object positions,
 ↪ but create questions and
 Chain-of-Thought (CoT) as if analyzing the first image.
4. Only ask questions relevant to their actual spatial
 ↪ relationship:
 - If objects are primarily horizontally separated: ask about
 ↪ left/right, not up/down/front/back.
 - If objects are primarily vertically separated: ask about
 ↪ up/down, not left/right/front/back.
5. Additional questions can be about distance, alignment, or
 ↪ blocking.
6. Use the actual object names in questions, not [A] [B] codes.
7. For each question, provide the correct answer (yes/no).
8. For each question, provide a CoT with two steps: first identify
 ↪ the bounding box coordinates
 from the first image, then briefly describe the spatial
 ↪ relationship.

Format your response as a JSON list of objects with 'question',
 ↪ 'answer', and 'cot' fields.

Single-Image Spatial Reasoning Prompt.

System Prompt

You are looking at an image with labeled objects and their bounding
 ↪ box coordinates:
 {object_labels}.

Please generate spatial relationship questions following these
 ↪ rules:

1. Generate 2-3 questions about the spatial relationship between
 ↪ the {obj1} and the {obj2}.
2. Use the coordinate information to understand object positions,
 ↪ but create questions and
 CoT as if analyzing a natural image.
3. Only ask questions relevant to their actual spatial
 ↪ relationship.
4. Use the actual object names in questions, not [A] [B] codes.
5. For each question, provide the correct answer (yes/no).
6. For each question, provide a CoT with two steps: first identify
 ↪ the bounding box
 coordinates, then briefly describe the spatial relationship.

Format your response as a JSON list of objects with 'question',
 ↪ 'answer', and 'cot' fields.

G.2 WHERE2PLACE SPATIAL LAYOUT PREDICTION**System Prompt**

You are an agent who reasons about free space and spatial
 ↪ relations. Based on the given image
 and prompt, your task is to output a tuple (min_x, min_y, max_x,
 ↪ max_y) that represents the
 bounding box of the object or region in the image that best matches
 ↪ the description in the
 prompt. min_x, min_y, max_x, max_y should be integers indicating
 ↪ pixel locations. Do not
 include any additional text in your answer other than the tuple
 ↪ (min_x, min_y, max_x, max_y).

User Prompt

Here is an image whose dimensions are labeled on the side.
 ↪ {question_text}

G.3 MULTI-ROBOT VIEW ANALYSIS**System Prompt**

You are analyzing two images from different robot perspectives
 ↪ viewing the same environment.
 These images represent two distinct robot viewpoints that may show
 ↪ overlapping or complementary
 parts of the scene. **IMPORTANT FORMAT REQUIREMENTS:**

1. ALL reasoning must be enclosed within <think> </think> tags.
2. When identifying objects RELEVANT TO THE QUESTION, provide their
 ↪ bounding box coordinates
 in the format: [x1, y1, x2, y2].
3. Only include bounding boxes for objects directly related to
 ↪ answering the question.

4. The final numerical answer MUST be placed in `\boxed{NUMBER}` -
 ↪ put ONLY the number inside the braces.
5. Do NOT put coordinates, lists, or other content inside `\boxed{}`.

EXAMPLE FORMAT:

`<think>`

I need to analyze both robot perspectives to count the requested
 ↪ objects.

In the main image, I can see a cup at bounding box [123, 150, 212,
 ↪ 250] and another cup at [215, 100, 122, 180].

In the auxiliary image, I can see one cup at [150, 200, 250, 311].
 Combining both perspectives, I count 3 cups total.

`</think>`

`\boxed{3}`

User Message Format.

User Message

```
main picture: <image>
auxiliary picture: <image>
Question: {object_counting_question}
```

H CASE STUDIES

E2W-1: What is the count of Pizza in the scene?



Figure 5: Example of an E2W-1 sample (Case 1). Two ego-centric views of a kitchen scene are provided, and the model must count the total number of pizzas by resolving cross-view object correspondences.

Model Responses (Case 1: Pizza Counting)

Ground truth answer: `\boxed{3}`

Our model (correct):

Our model: <think>\nI need to analyze images from two robot
 ↪ perspectives to answer the question about 'How many pizza
 ↪ do you observe?'.\n\nLet me first examine the main
 ↪ perspective (Image A):\n- I can see the first pizza at
 ↪ [419, 204, 451, 224]\n- I also see a second pizza at
 ↪ [532, 94, 571, 102]\n\nNow examining the auxiliary
 ↪ perspective (Image B):\n- In this view, I can see the
 ↪ first pizza at [0, 253, 44, 280]\n- I also notice a
 ↪ second pizza located at [499, 218, 544, 238]\n-
 ↪ Additionally, there's a third pizza at [161, 101, 200,
 ↪ 110]\n\nAnalyzing spatial correspondence between the two
 ↪ perspectives:\n- pizza_0 visible in main perspective at
 ↪ [419, 204, 451, 224] corresponds to the same object
 ↪ visible in auxiliary perspective at [0, 253, 44, 280]\n-
 ↪ pizza_1 at [499, 218, 544, 238] in auxiliary perspective
 ↪ is not visible in main perspective\n- pizza_2 visible in
 ↪ main perspective at [532, 94, 571, 102] corresponds to
 ↪ the same object visible in auxiliary perspective at [161,
 ↪ 101, 200, 110]\n\nCombining observations from both
 ↪ perspectives, the total number of objects you asked me to
 ↪ count is 3.\n</think>\n\n\boxed{3}

GPT-5 (incorrect, predicts 2):

Gpt-5: I can see two pieces of pizza:
 One slice on the upper wooden shelf (visible in both images).
 One slice on the counter near the barstools.
 The item on the stove looks like a roasted chicken or meat,
 ↪ not pizza.
 So the answer is: 2 pizzas (slices).

Qwen-max (incorrect, predicts 2):

Qwen-max: Based on the two images provided, I can observe a
 ↪ total of two pizzas.
 Here is the breakdown:
 One pizza is on the stovetop in the first image and remains
 ↪ there in the second image.
 A second pizza is visible on the kitchen island in the second
 ↪ image. It appears to be sitting next to an open cardboard
 ↪ box, likely a pizza box.
 Therefore, across both views of the kitchen, there are 2
 ↪ pizzas visible.

E2W-2: What do you see as the third item from the left on the table?



Figure 6: Example of an E2W-2 sample (Case 2). The model receives two views of a table scene and must identify the third item from the left by integrating spatial information across views.

Model Responses (Case 2: Third Item on Table)

Ground truth answer: `bread`

Our model (correct):

Our model: <think>\nI need to analyze images from two robot
 ↪ perspectives to answer the spatial reasoning question:
 ↪ 'What do you see as the third item from the left on the
 ↪ table?'.\n\nLet me first examine the main perspective
 ↪ (Image A):\n- I can see a cardboardbox located at [150,
 ↪ 113, 183, 129]\n- There's a scissors positioned at
 ↪ coordinates [283, 112, 318, 130]\n- I notice a bread at
 ↪ [321, 128, 381, 147]\n\nSpatial relationships in the main
 ↪ perspective:\n- cardboardbox is to the left of scissors
 ↪ (distance: 134.0 pixels)\n- cardboardbox is to the left
 ↪ of bread (distance: 185.2 pixels)\n- scissors is to the
 ↪ left of bread (distance: 53.1 pixels)\n\nNow examining
 ↪ the auxiliary perspective (Image B):\n- I can see a
 ↪ scissors located at [54, 115, 90, 135]\n- There's a bread
 ↪ positioned at coordinates [48, 132, 99, 152]\n- I notice
 ↪ a tomato at [175, 115, 188, 127]\n\nSpatial relationships
 ↪ in the auxiliary perspective:\n- scissors is near bread
 ↪ (distance: 17.1 pixels)\n- scissors is to the left of
 ↪ tomato (distance: 109.6 pixels)\n- bread is to the left
 ↪ of tomato (distance: 110.0 pixels)\n\nAnalyzing spatial
 ↪ correspondence between the two perspectives:\n-
 ↪ cardboardbox is only visible in main perspective at [150,
 ↪ 113, 183, 129]\n- scissors is visible in both
 ↪ perspectives at [283, 112, 318, 130] and [54, 115, 90,
 ↪ 135] respectively\n- bread is visible in both
 ↪ perspectives at [321, 128, 381, 147] and [48, 132, 99,
 ↪ 152] respectively\n- tomato is only visible in auxiliary
 ↪ perspective at [175, 115, 188, 127]\n\nTherefore, the
 ↪ answer to 'What do you see as the third item from the
 ↪ left on the table?' is bread.\n</think>\n\n\\boxed{bread}

GPT-5 (incorrect, predicts tomato):

Gpt-5: On the table, from left to right in the images, I see:
 A loaf of bread
 A pair of scissors
 A tomato
 So the third item from the left is a tomato.

Qwen-max (incorrect, focuses on tomato in second image):

Qwen-max: Based on the two images provided, the items on the
 ↪ table appear to have been rearranged.
 Let's analyze each image:
 In the first image: Looking from left to right on the white
 ↪ table, we can identify:
 A small brown cardboard box.
 A pair of yellow-handled scissors.
 A loaf of bread.
 Therefore, in the first image, the third item from the left
 ↪ is the loaf of bread.
 In the second image: The arrangement has changed. From left
 ↪ to right, we see:
 The loaf of bread.
 The yellow-handled scissors.

A single red tomato in the center of the table.
 Therefore, in the second image, the third item from the left
 ↪ is the tomato.
 Since you asked "what do you see," and presented two
 ↪ different views, it's important to note the difference.
 ↪ However, if we consider the most complete or final view,
 ↪ the second image shows a more organized setup with the
 ↪ tomato placed centrally.
 The third item from the left on the table in the second image
 ↪ is a tomato.

E2W-3: Please grasp the things in the left of banana

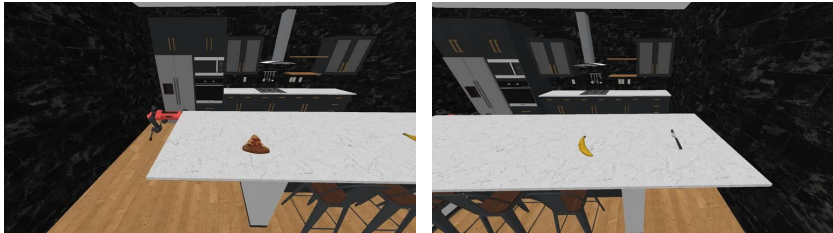


Figure 7: Example of an E2W-3 sample. The model receives two ego-centric views from different robot perspectives and must localize the target object—in this case, the pizza—and output the precise grasp location. Solving the task requires cross-view object correspondence, reasoning about spatial ordering, identifying the visible target in each view, and determining the final grasp coordinate in the main perspective.

Model Responses (Case 3: E2W-3 Grasp Localization)

Our model:

Our model: <think>\nI need to analyze images from two robot
 ↪ perspectives to determine
 the precise grasping location for the instruction:
 'Please grasp the things in the left of banana.'.\n\n

Let me first examine the main perspective (Image A):\n
 - I can see a banana located at [742, 243, 767, 258] with
 ↪ center at [754.5, 250.5]\n
 - There's a pizza positioned at coordinates [440, 246, 495,
 ↪ 281]
 with center at [467.5, 263.5]\n\n

Spatial arrangement from left to right in main perspective:\n
 - Position 1: pizza at center [467.5, 263.5]\n
 - Position 2: banana at center [754.5, 250.5]\n\n

Now examining the auxiliary perspective (Image B):\n
 - I can see a banana at [272, 248, 299, 286], center [285.5,
 ↪ 267.0]\n
 - There's a knife at [445, 235, 466, 272], center [455.5,
 ↪ 253.5]\n\n

Overlap number = 1. Spatial ordering:\n
 - Position 1: banana\n

```
- Position 2: knife\n\n
```

```
Analyzing target object:\n
```

```
The target is the pizza, which is left of the banana in the  
↔ main perspective.\n\n
```

```
Pizza bounding box: [440, 246, 495, 281]\n
```

```
Center = [467.5, 263.5]\n\n
```

```
Thus I should grasp at image 0 coordinates [467.5, 263.5].\n
```

```
</think>\n\n
```

```
\\boxed{0, [467.5, 263.5]}
```